



## Competitive removal of $\text{Cu}^{2+}$ , $\text{Cd}^{2+}$ , $\text{Zn}^{2+}$ , and $\text{Ni}^{2+}$ ions onto iron oxide nanoparticles from wastewater

Shahlaa E. Ebrahim<sup>a,\*</sup>, Abbas H. Sulaymon<sup>b</sup>, Hasanain Saad Alhares<sup>a</sup>

<sup>a</sup>College of Engineering, University of Baghdad, Baghdad, Iraq, Tel. +964 07707947617; email: [shahlaa.ebrahim@fulbrightmail.org](mailto:shahlaa.ebrahim@fulbrightmail.org) (S.E. Ebrahim), Tel. +964 07901147074; email: [hassanian73@yahoo.com](mailto:hassanian73@yahoo.com) (H. Saad Alhares)

<sup>b</sup>Mechanical Engineering Department, Islamic College University, Al Najaf, Iraq, Tel. +964 07903971195; email: [inas\\_abbas@yahoo.com](mailto:inas_abbas@yahoo.com)

Received 30 March 2015; Accepted 16 October 2015

### ABSTRACT

A competitive adsorption of  $\text{Cu}^{2+}$ ,  $\text{Ni}^{2+}$ ,  $\text{Zn}^{2+}$ , and  $\text{Cd}^{2+}$  ions onto  $\text{Fe}_3\text{O}_4$  nanomaterial was studied. Experimental parameters such as, pH, initial metal concentrations, and temperatures were investigated. The uptake capacity was 11.5, 6.07, 11.1, and 9.68 mg/g for  $\text{Cu}^{2+}$ ,  $\text{Ni}^{2+}$ ,  $\text{Zn}^{2+}$ , and  $\text{Cd}^{2+}$ , respectively. The optimum pH and contact time were found to be 6 and 50 min for  $\text{Cu}^{2+}$ ,  $\text{Ni}^{2+}$ ,  $\text{Zn}^{2+}$ , and  $\text{Cd}^{2+}$ . The equilibrium isotherm for single component system was of favorable type and Freundlich isotherm model gave the best fitting for the experimental data. Binary, ternary, and quaternary systems were conducted to find the adsorption isotherm constants for each adsorption models; combination of Langmuir–Freundlich model gave the best fit. In single, binary, ternary, and quaternary systems,  $\text{Cu}^{2+}$  always adsorbed more favorably onto nanosorbent than  $\text{Zn}^{2+}$ ,  $\text{Cd}^{2+}$ , and  $\text{Ni}^{2+}$ . The adsorption capacity parameters were:  $\text{Cu}^{2+} > \text{Zn}^{2+} > \text{Cd}^{2+} > \text{Ni}^{2+}$ . Thermodynamic study was carried out and the results showed that the adsorption was an endothermic process.

*Keywords:* Adsorption; Heavy metals; Ions; Competitive; Nanosorbent

### 1. Introduction

Rapid industrialization and urbanization has resulted in the deterioration of water, air, and land quality. A tremendous increase in the use of heavy metals over the past few decades has inevitably resulted in an increased flux of metallic substances in the aquatic environment. Heavy metals get distinguished from other toxic pollutants due to their non-biodegradability [1–4].

Presences of heavy metals in wastewaters cause significant environmental problems. High concentra-

tions of heavy metals are known to be toxic and carcinogenic to living organisms. When heavy metals are presented even in a very low concentration, their concentration may be elevated through bio-magnification to a level that they start to exhibit toxic characteristics. Therefore, heavy metals are major pollutants in many industrial wastewaters and are toxic to human and aquatic life [5]. Due to their elemental non-degradable nature, heavy metals always and regardless of their chemical form, pose serious ecological risk, when released into the environment. The metals which are of greatest environmental concern are cadmium, mercury, lead, chromium, cobalt, copper, nickel, and zinc [6]. The presence of heavy metal ions

\*Corresponding author.

in the environment has been a matter of major concern due to their toxicity to human life. Unlike organic pollutants, the majority of which are susceptible to biological degradation, heavy metal ions will not degrade into harmless end products. Heavy metal ions such as cobalt, copper, nickel, chromium, mercury, lead, cadmium, and zinc ions are detected in the waste streams from different industrial activities such as mining operations, tanneries, electronics, electroplating, petroleum refineries, and petrochemical industries [7].

The toxicity of heavy metals can be listed in order of decreasing toxicity as  $\text{Hg} > \text{Cd} > \text{Cu} > \text{Zn} > \text{Ni} > \text{Pb} > \text{Cr} > \text{Al} > \text{Co}$ , although this is only approximate as the vulnerability of species to individual metals varies. Toxicity also varies according to environmental conditions that control the chemical speciation of the metals [8,9].

The removal of heavy metals ions from wastewater involves high-cost techniques such as ion exchange, evaporation, precipitation, and membrane separation. However, these common techniques are too expensive to treat low levels of heavy metals in wastewater. Adsorption techniques are widely used in the field of removing small quantities of pollutant present in large volume of fluid, which can be carried out in batch or continuous operation [10]. Many factors that affect the decision of choosing an adsorbent for removal of pollutants from water such as: cost of the adsorbent, abundance, availability, and effectiveness of the adsorbent [11].

The last decade has seen a continuous improvement in the development of effective noble adsorbents in the form of activated carbon [12], zeolites [13], clay minerals [14], chitosan [15], lignocelluloses [16], natural inorganic minerals [17], and functionalized polymers [18]. However, most of these adsorbents are either not effective (due to diffusion limitation or the lack of enough active surface sites) or have shown problems such as high cost, of separation from wastewater, or generation of secondary wastes. Recently nanoadsorbents viz. nanoalumina [19], functionalized carbon nanotubes [20], and hydroxyapatite nanoparticles [21], have demonstrated high-adsorption efficiency for metal ions removal. The utilization of iron oxide nanomaterials has received much attention due to their unique properties, such as extremely small size, high surface-area-to-volume ratio, surface modifiability, and excellent magnetic properties [22]. Such adsorbent combining nanotechnology and magnetic separation technique has not only demonstrated high adsorption efficiency, but have also shown additional benefits such as ease of synthesis, easy recovery and manipulation via subsequent coating and functionalization, absence of secondary pollutants, cost-effectiveness, and

environmental friendliness [23]. Till date, several magnetic nanomaterials, including maghemite nanoparticles [24],  $\text{Fe}_3\text{O}_4$  magnetic nanoparticles [25], and  $\text{Fe}_3\text{O}_4$  nanoparticles functionalized and stabilized with compounds such as humic acid [26] have been explored for the removal of metal ions. In the present study, iron oxide nanosorbent was used for the competitive removal of  $\text{Cu}^{2+}$ ,  $\text{Cd}^{2+}$ ,  $\text{Ni}^{2+}$ , and  $\text{Zn}^{2+}$  in batch reactors at different operating conditions.

## 2. Equilibrium isotherm batch models for nanosorbent

### 2.1. Single component system

#### 2.1.1. Langmuir model (1916)

The Langmuir model can be represented as:

$$q_e = \frac{q_{\max} b C_e}{(1 + b C_e)} \quad (1)$$

where  $q_e$  is the amount of adsorbate adsorbed per mass of adsorbent (mg/g).  $C_e$  is the equilibrium concentration (mg/L),  $q_{\max}$  corresponds to the maximum achievable uptake by a system, and  $b$  is related to the affinity between the sorbate and sorbent, (L/mg). The Langmuir constant " $q_{\max}$ " is often used to compare the performance of adsorbents; while the other constant " $b$ " characterizes the initial slope of the isotherm. Thus, for a good adsorbent, a high  $q_{\max}$  and a steep initial isotherm slope (i.e. high  $b$ ) are generally desirable [27,28].

The Langmuir model assumes the surface consists of adsorption sites, all adsorbed species interact only with a site and not with each other, adsorption is limited to a monolayer, and adsorption energy of all the sites is identical and independent of the presence of adsorbed species on neighboring sites [29].

Each component is adsorbed onto the surface according to ideal solute behavior; there is no interaction or competition between molecules involved under homogenous conditions [30].

The important characteristic of the Langmuir isotherm can be expressed in terms of dimensionless constant separation factor for equilibrium parameter  $R_L$ . This is defined by [6]:

$$R_L = \frac{1}{b + C_o} \quad (2)$$

[31] shows, using mathematical calculation, that the parameter  $R_L$  indicates the shape of isotherm:  $R_L > 1$  unfavorable,  $R_L = 1$  linear,  $R_L = 0$  irreversible and  $0 < R_L < 1$  favorable.

### 2.1.2. Freundlich model (1918)

The Freundlich isotherm can be represented as:

$$q = KC_e^{1/n} \quad n > 1 \quad (3)$$

The Freundlich isotherm was originally empirical in nature, but was later interpreted as the sorption to heterogeneous surfaces or surfaces supporting sites with various affinities. It is assumed stronger binding sites are initially occupied, and the binding strength decreasing with increasing degree of site occupation. It incorporates two constants:  $K$ , corresponds to the maximum binding capacity; and  $n$ , characterize the affinity between the sorbent and sorbate [32].

### 2.1.3. Redlich–Peterson model (1959)

$$q_e = \frac{K_{RP}C_e}{1 + a_{RP}C_e^{\beta_{RP}}} \quad (4)$$

Redlich–Peterson isotherm shows that an “area of stability” is reached after a frequent rise in the curve, i.e. several layers of adsorption occurs first. This isotherm assume equilibrium for heterogeneous surfaces as it contains the heterogeneity factor  $\beta$ , converges to Henry’s law at low surface coverage and thermodynamically consistent. However, it does not have as wide a practical application as the Langmuir and the Freundlich isotherms due to the inconvenience of evaluating three isotherm constants [33].

$\beta_{RP}$  has values between 0 and 1. For  $\beta_{RP} = 1$  the Redlich–Peterson model converts to the Langmuir model.  $\beta_{RP} = 0$  the Henry’s Law form results.

### 2.1.4. Sips model (1948)

$$q_e = \frac{K_s C_e^{\beta_s}}{1 + a_s C_e^{\beta_s}} \quad (5)$$

where  $K_s$ ,  $a_s$ , and  $\beta_s$  are constant. This equation is also called as Langmuir–Freundlich isotherm. At low-sorbate concentrations it effectively reduces to a Freundlich isotherm and thus does not obey Henry’s law. At high-sorbate concentrations, it predicts the monolayer sorption capacity characteristics of the Langmuir isotherm [34].

### 2.1.5. Khan model (1997)

$$q_e = \frac{q_{\max} b_k C_e}{(1 + b_k C_e)^{a_k}} \quad (6)$$

where  $b_k$  and  $a_k$  are constants  $q_{\max}$  maximum uptake [32].

### 2.1.6. Toth Model (1971)

$$q_e = \frac{q_{\max} b_T C_e}{\left[1 + (b_T C_e)^{\frac{1}{n_T}}\right]^{n_T}} \quad (7)$$

where  $b_T$  and  $n_T$  are constants [32].

It derives from potential theory and is used in heterogeneous systems. Toth model assumes a quasi-Gaussian energy distribution; most sites have adsorption energy lower than the peak of maximum adsorption energy [35].

## 2.2. Multicomponent systems

The adsorption of the solute of interest not only depends on the adsorbent surface properties and physical–chemical parameters of a solution such as pH and temperature, but also on the number of solutes and their concentrations. In such cases, the adsorption will become competitive, with one solute competing with another to occupy the binding sites [36].

For binary solute cases, different isotherm models have been used to correlate single-solute isotherm data and to describe multisolute sorption isotherms based on the time-consuming iterative algorithm [37].

### 2.2.1. Extended Langmuir model (ELM)

$$q_i = \frac{b_i q_{m,i} C_{e,i}}{\left(1 + \sum_{j=1}^n b_j C_{e,j}\right)} \quad (8)$$

where  $C_{e,i}$  is the equilibrium concentration of the component  $i$  in the multicomponent solution,  $q_i$  is the equilibrium uptake of the component  $i$ ,  $b_i$ , and  $q_{m,i}$  are the Langmuir isotherm model parameters obtained suitably from Eq. (1) in the single solute system. This model assumes homogeneous surface with respect to the energy of sorption, no interaction between adsorbed species and that all sorption sites are equally available to all adsorbed species [27].

### 2.2.2. Redlich–Peterson model

The three parameter isotherm of Redlich–Peterson that has been empirically developed for multicomponent mixtures is [38,39]:

$$q_i = \frac{K_{R,i} q_{m,i} C_{e,i}}{\left(1 + \sum_{j=1}^n a_{R,j} C_{e,j}^{B,j}\right)} \quad (9)$$

where  $K_{R,i}$  and  $q_{m,i}$  are the Redlich–Peterson isotherm model parameter obtained from Eq. (4) for single solute system.

### 2.2.3. Combination of Langmuir–Freundlich model

The competitive model related to individual isotherms parameters are expressed in the following equation [40]:

$$q_i = \frac{q_{m,i} b_i C_{ei}^{\left(\frac{1}{n_i}\right)}}{\left(1 + \sum_{j=1}^n b_j C_{ej}^{\left(\frac{1}{n_j}\right)}\right)} \quad (10)$$

## 3. Experimental work and materials

The present study is to evaluate the competitive adsorption of heavy metals from wastewater onto nanosorbent ( $\text{Fe}_3\text{O}_4$ ) in batch reactor at different operating conditions in single, binary, ternary, and quaternary system.

### 3.1. Materials

#### 3.1.1. Adsorbate (stock solutions)

A stock solution of copper, zinc, nickel, and cadmium ions with a concentration of (1,000 mg/L) was prepared using  $\text{Cu}(\text{NO}_3)_2$ ,  $\text{Cd}(\text{NO}_3)_2$ ,  $\text{Ni}(\text{NO}_3)_2$ , and  $\text{Zn}(\text{NO}_3)_2$  (minimum purity 99.5%). Table 1 shows the main physicochemical properties of the metals. A 3.805, 2.744, 4.945, and 4.548 g of copper nitrate, cadmium nitrate, nickel nitrate, and zinc nitrate, respectively, were each dissolved in 200 ml of distilled water. A 10-ml concentrated  $\text{HNO}_3$  was added and diluted to 1,000 ml with distilled water [41]. Concentrations of 50 ppm from these salts were used as adsorbate for different weights of nanosorbent. Flame atomic absorption spectrophotometer (Buck, Accusys 211, USA) was used for measuring metal concentrations.

#### 3.1.2. Nanosorbent

( $\text{Fe}_3\text{O}_4$ ) nanoparticles (US Research Nanomaterials, Inc., Houston, TX 77084, USA) were used. The main physical properties of the nanoparticules are listed in Table 2, certificate of analysis—% of iron oxide nanoparticules is: Ca 0.0229% <, Cr 0.0016% <, K 0.0012% <, Mg 0.086% <, and  $\text{SiO}_2$  0.0142% <. Fig. 1 shows scanning electron micrographs for nanosorbent which carried out in Nano Research Center/(University of Technology)/Baghdad—Iraq.

### 3.2. Experimental work

#### 3.2.1. Determination of optimum pH

The effect of pH on  $\text{Cu}^{2+}$ ,  $\text{Zn}^{2+}$ ,  $\text{Ni}^{2+}$ , and  $\text{Cd}^{2+}$  ions adsorption onto nanosorbent was studied; 0.5 g of  $\text{Fe}_3\text{O}_4$  was placed in a volumetric flasks and mixed with 100 ml of single metal ion solutions with concentration of 50 mg/L of  $\text{Cu}^{2+}$ ,  $\text{Zn}^{2+}$ ,  $\text{Ni}^{2+}$ , and  $\text{Cd}^{2+}$  ions, respectively. These were maintained at different pH values ranging from 3 to 7 using 0.1 M NaOH or  $\text{HNO}_3$  solution at agitation speed of 200 rpm for a period of 30 min and at room temperature [43]. Separation of nanosorbents from aqueous solution was achieved using a small horseshoe magnet. Samples (10 ml) were taken from each volumetric flask and measured using AAS.

#### 3.2.2. Equilibrium isotherm experiments

Different weights of nanosorbent were used (0.05, 0.1, 0.2, 0.4, 0.6, 0.8, 1, 1.2, and 1.4 g) and placed in nine volumetric flasks of 250 ml. A sample of 100 ml of 50 mg/L was added to each flask for single systems of  $\text{Cu}^{2+}$ ,  $\text{Zn}^{2+}$ ,  $\text{Ni}^{2+}$ , and  $\text{Cd}^{2+}$ , respectively. The pH of the metal solutions was adjusted to the optimum pH value using 0.1 M NaOH or 0.1 M  $\text{HNO}_3$ . The flasks were then placed on a shaker (HV-2 ORBTAL, Germany) and agitated continuously for 50 min at 200 rpm. Few drops of 0.1-M  $\text{HNO}_3$  were added to samples after separation of nanosorbent from aqueous solution to decrease the pH value below two in order to fix the concentration of the heavy metals during storage [41]. Concentrations were measured by means of the residual concentrations of zinc, cadmium, copper, and nickel ions. The adsorbed amount is calculated using the following equation:

$$q_e = \frac{V_1(C_0 - C_e)}{W_{(\text{nanosorbent})}} \quad (11)$$

The adsorption isotherms were obtained by plotting the weight of solute adsorbed per unit weight of biomass ( $q_e$ ) against the equilibrium concentration of the solute in the solution ( $C_e$ ) [32].

#### 3.2.3. Thermodynamic parameters of adsorption

The effect of temperature on  $\text{Cu}^{2+}$ ,  $\text{Zn}^{2+}$ ,  $\text{Cd}^{2+}$ , and  $\text{Ni}^{2+}$  ions adsorption uptake onto nanosorbent was studied. About 0.6 g of nanosorbent was mixed with 100 ml of single metal ion solutions with concentration of 50 mg/L of  $\text{Cu}^{2+}$ ,  $\text{Zn}^{2+}$ ,  $\text{Cd}^{2+}$ , and  $\text{Ni}^{2+}$ , respectively. These were maintained at different

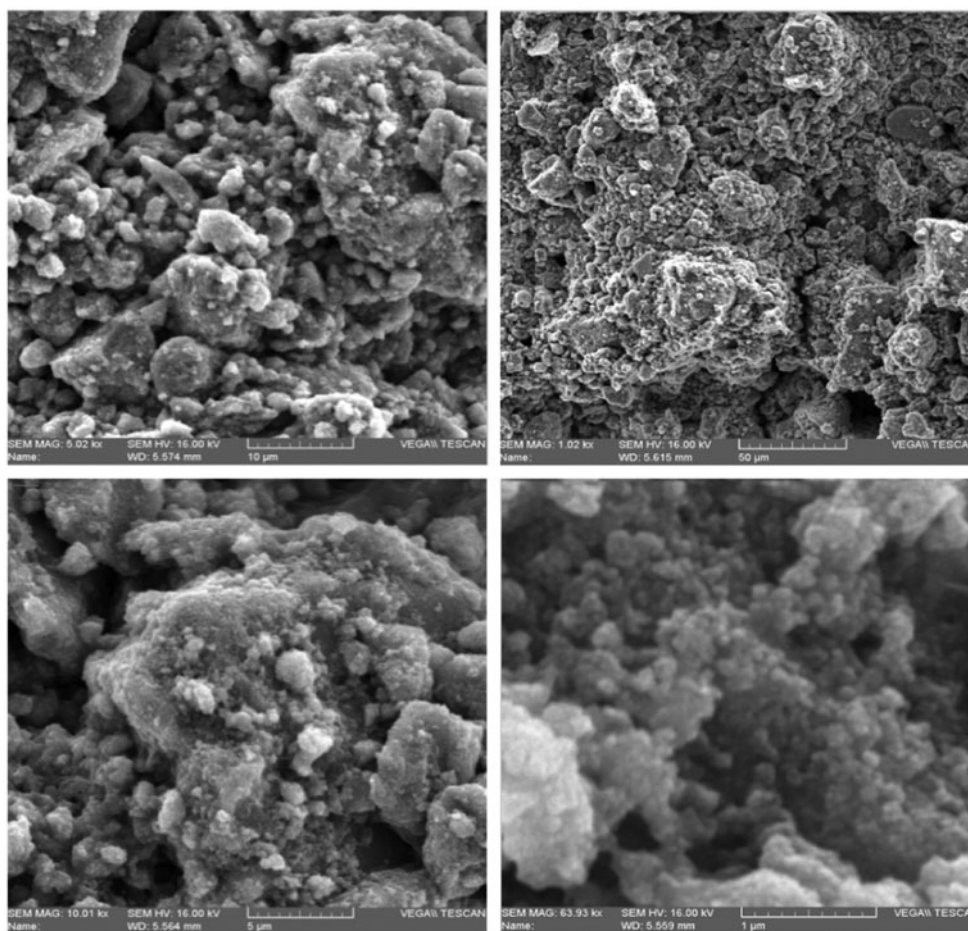


Fig. 1. Scanning electron micrographs for nanosorbent.

temperature values ranging from 20 to 50°C for a period of 50 min, agitation speed was 200 rpm. Samples (10 ml) were taken from each volumetric flask and measured using AAS.

## 4. Results and discussion

### 4.1. Batch system

#### 4.1.1. Effect of pH

Fig. 2 shows the effect of pH (3, 4, 5, 6, 7) on the adsorption uptake of  $\text{Cu}^{2+}$ ,  $\text{Ni}^{2+}$ ,  $\text{Zn}^{2+}$ , and  $\text{Cd}^{2+}$  ions.

The pH value above 6.0 must be avoided; this is due to the insoluble metal hydroxides which makes the true sorption studies impossible [10]. At low pH around 2, proton would compete for active binding sites with metal ions. The protonation of active sites thus tends to decrease the metal sorption [42]. Therefore, optimum copper, nickel, zinc, and cadmium ions adsorption process will be at pH 6 as shown in Fig. 2. These results agreed with the results obtained by [43,44].

#### 4.1.2. Effect of contact time

About 0.6 g of  $\text{Fe}_3\text{O}_4$  was mixed with 100 ml of single metal ion solutions concentration of 50 mg/L of  $\text{Cu}^{2+}$ ,  $\text{Ni}^{2+}$ , and  $\text{Cd}^{2+}$  ions at pH 6. These were agitated at different periods (10, 20, 30, 40, 50, 60, and 70 min). Fig. 3 shows the results of removal efficiency (%) with the contact time. It can be concluded that 50 min contact time is sufficient to reach equilibrium condition for all heavy metals.  $\text{Fe}_3\text{O}_4$  nanoadsorbent is a nonporous adsorbent, as confirmed by surface area and porosity measurement, where only external adsorption occurs. This type of adsorption mass transfer requires less time to reach equilibrium. This result is promising as equilibrium time plays a major role in wastewater treatment plant economic viability [43].

#### 4.1.3. Effect of initial heavy metal concentration

Fig. 4 shows the removal efficiency with different concentrations of 10, 50, 100, and 150 mg/L. It can be seen that the percentage removal efficiency was not

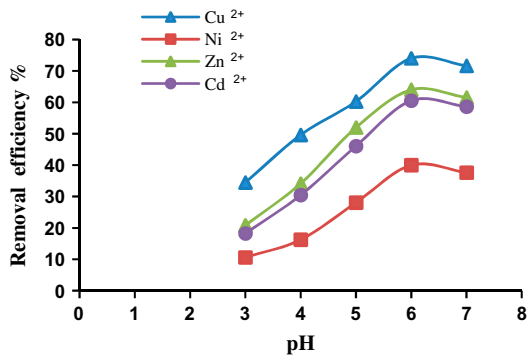


Fig. 2. Effect of different pH values on copper, zinc, nickel, and cadmium ions uptake onto nanosorbents,  $C_o = 6 \text{ g/l}$ ,  $C_o = 50 \text{ mg/L}$ , 200 rpm,  $W = 0.6 \text{ g}$ .

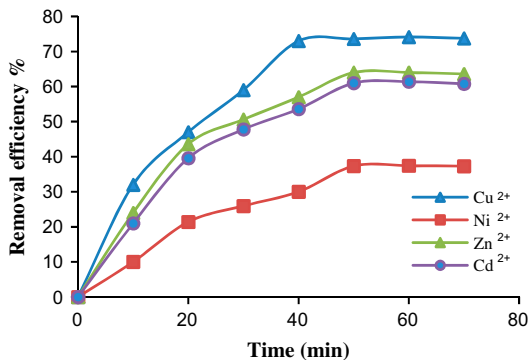


Fig. 3. Adsorption efficiency for nanosorbent with different contact time,  $C_o = 50 \text{ ppm}$ , pH 6,  $W = 0.6 \text{ g}$ , 200 rpm.

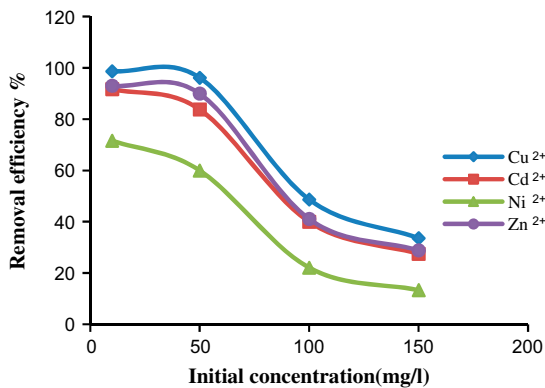


Fig. 4. Percentage of removal adsorption efficiency with variation of initial concentration, contact time 50 min, 200 rpm, pH 6, and  $W = 1 \text{ g}$ .

altered greatly if the concentration increase from 10 to 50 mg/L, this behavior due to that 1 g of nanosorbent may contain enough sites for this concentration range,

but when the concentrations increase to 100 and 150 mg/L the sites will not be enough to accumulate these concentrations so that the reduction in percentage removal efficiency was obvious. These results agreed with the results obtained by [32,43].

#### 4.1.4. Effect of temperature and thermodynamic parameters

The effect of temperature on the equilibrium sorption capacity for  $\text{Cu}^{2+}$ ,  $\text{Ni}^{2+}$ ,  $\text{Zn}^{2+}$ , and  $\text{Cd}^{2+}$  ions has been investigated at temperature range between 20 and 50°C. Fig. 5 shows the variation of percentage removal efficiency with temperature.

It can be concluded that the increase in temperature leads to the increase in percentage removal efficiency, and the variation of temperature from 20 to 30°C has little effect on the adsorption process, so that the adsorption experiments can be carried out at room temperature without any adjustment. These results agreed with the results obtained by [22,43].

Thermodynamic parameters ( $\Delta G^\circ$ ,  $\Delta H^\circ$ , and  $\Delta S^\circ$ ) were obtained by varying the temperature and calculated using the following equation:

$$\Delta G = -RT \ln(K_c) \quad (12)$$

where

$$K_c = \frac{C_{ad}}{C_e} \quad (13)$$

where  $K_c$  is the equilibrium constant,  $C_{ad}$  is the amount of metal adsorbed onto adsorbent per liter of the solution at equilibrium (mg/L),  $C_e$  is the

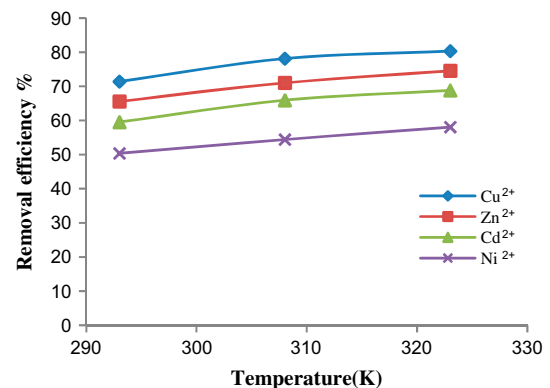


Fig. 5. Variation of percentage removal with solution temperature,  $C_o = 50 \text{ mg/L}$ , contact time 50 min,  $W = 0.6 \text{ g}$ , and 200 rpm.

equilibrium concentration of the metal in the solution (mg/L),  $T$  is absolute temperature (K), and  $R$  is the universal gas constant (8.314 J/mol K). In addition, enthalpy changes ( $\Delta H$ ) and entropy changes ( $\Delta S$ ) can be estimated by the following equation [45]:

$$\Delta G = \Delta H - \Delta ST \quad (14)$$

The thermodynamic parameters, Gibbs free energy change ( $\Delta G^\circ$ ), standard enthalpy change ( $\Delta H^\circ$ ), and standard entropy change ( $\Delta S^\circ$ ) used to understand the effect of temperature on the adsorption [46].

The positive values of  $\Delta H^\circ$  reveal the adsorption is endothermic and physical in nature. Generally, the change in adsorption enthalpy for physisorption is in the range of  $-20$ – $40$  kJ mol $^{-1}$ , but chemisorptions are between  $-400$  and  $-80$  kJ mol $^{-1}$  [47]. Fig. 6 and Table 3 show the thermodynamic constants of adsorption obtained for Cu $^{2+}$ , Zn $^{2+}$ , Ni $^{2+}$ , and Cd $^{2+}$  ions onto nanosorbents.

Examining Table 3, it can be seen that the enthalpies were 12.8, 7.119, 11.25, and 10.59 kJ mol $^{-1}$  for Cu $^{2+}$ , Ni $^{2+}$ , Zn $^{2+}$ , and Cd $^{2+}$  ions, respectively, reveal the adsorption is endothermic and physical in nature. This is also supported by the increase in the values of uptake capacity of nanosorbents with the rise in temperature.

The positive values of entropies were 0.051, 0.043, 0.024, and 0.039 J mol $^{-1}$  K $^{-1}$ , and they reflect the affinity of Cu $^{2+}$ , Zn $^{2+}$ , Ni $^{2+}$ , and Cd $^{2+}$  ions to be adsorbed onto nanosorbent [48].

The decrease in the value of the free energy with the increase in temperature indicates that the adsorption process is endothermic and it is thereby favored with the increase in temperature, thus, the process is better carried out at high temperature [46].

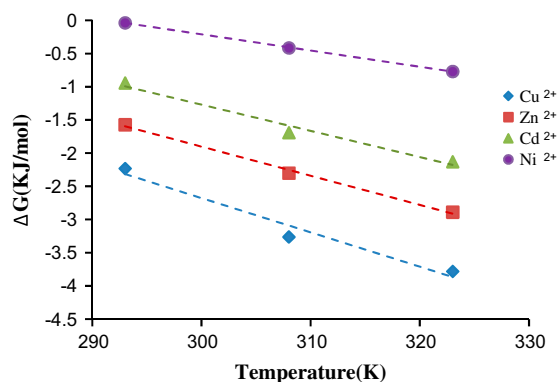


Fig. 6. Change of free energy with temperature for the adsorption of Cu $^{2+}$ , Zn $^{2+}$ , Ni $^{2+}$ , and Cd $^{2+}$  ions by nanosorbent at initial concentration of 50 mg/L and pH 6.

#### 4.1.5. Single component system

The adsorption isotherm of single component systems of Cu $^{2+}$ , Ni $^{2+}$ , Zn $^{2+}$ , and Cd $^{2+}$  ions, onto nanosorbent are shown in Fig. 7. The data were correlated with six models and the parameters for each model obtained from nonlinear statistical fit of the experimental data (STATISTICA software, version 6) as shown in Table 4. Figs. 8–11 show the comparison of Freundlich, Langmuir, Redlich–Peterson, Sips, Khan, and Toth models for copper, nickel, zinc, and cadmium ions, respectively.

Figs. 7–11 and Table 4 show the following:

- (1) Freundlich model gave the best fit of the experimental data for copper, nickel, zinc, and cadmium ions recognized by the highest values of ( $R^2$ ). This model has been used successfully to describe equilibrium adsorption. Results showed that maximum capacity and ( $n$ ) parameters are in the sequence as Cu $^{2+}$  > Zn $^{2+}$  > Cd $^{2+}$  > Ni $^{2+}$ .

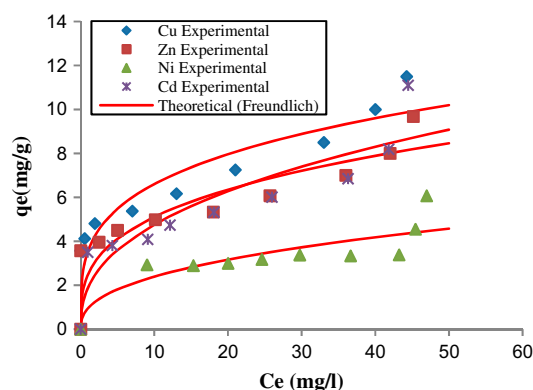


Fig. 7. Adsorption isotherms of Cu, Zn, Ni, and Cd ions onto nanosorbent,  $C_o = 50$  mg/L.

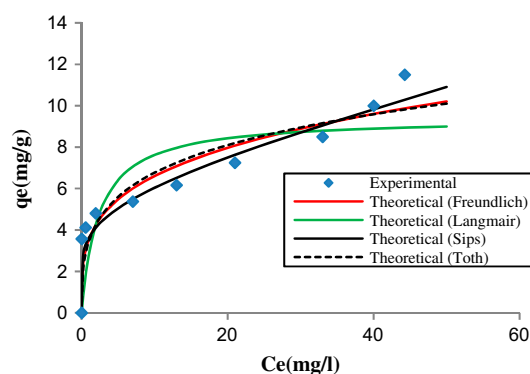


Fig. 8. Comparison of isotherm models for adsorption copper ions onto nanosorbent,  $C_o = 50$  mg/L.

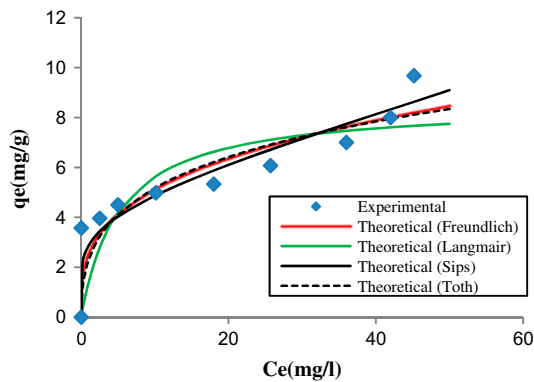


Fig. 9. Comparison of isotherm models for adsorption zinc ions onto nanosorbent,  $C_0 = 50$  mg/L.

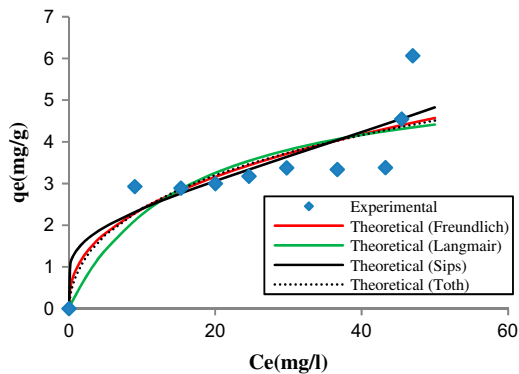


Fig. 10. Comparison of isotherm models for adsorption nickel ions onto nanosorbent,  $C_0 = 50$  mg/L.

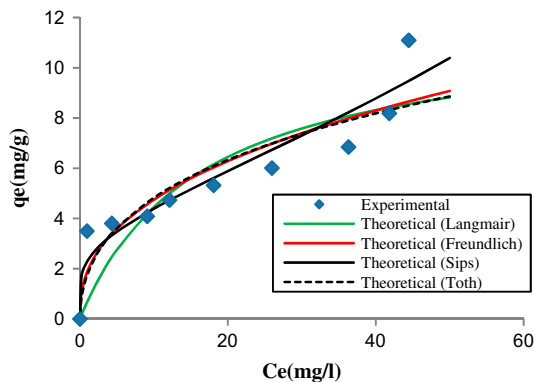


Fig. 11. Comparison of isotherm models for adsorption cadmium ions onto nanosorbent,  $C_0 = 50$  mg/L.

- (2) The equilibrium isotherm for each component is of favorable type  $n > 1$ .
- (3) The greater adsorption capacity was obtained at lower adsorbent dose. The higher removal rate was achieved at higher adsorbent dose.

- (4) Copper and zinc ions which have the highest affinity order for being adsorbed by the nanosorbent, have the lowest hydration van der Waals' radius while nickel ions have the least favorable by the nanosorbent, and the highest hydration van der Waals' radius, (as shown in Table 1). This coincides with the fact that less-hydrated ions radius is preferably accumulated at interface [49].
- (5) Sharing of electrons is involved in covalent binding. The binding strength increases with increasing polarizability of the ions [50]. From Table 1 the electronegativities for copper is higher than zinc, therefore, copper ions has higher strength of covalent binding than the lower affinity metals ions (zinc, cadmium, and nickel). As the electronegativity of the atom increases, its ionic forms seem to be more easily sorbed by the adsorbent [51].

#### 4.1.6. Binary component system

The data were correlated with three models (Extended Langmuir, Redlich–Peterson, and Combination of Langmuir–Freundlich). The parameters for each model obtained from nonlinear statistical fit of the experimental data were shown in Table 5. The adsorption isotherms for binary component systems of  $\text{Cu}^{2+}$ ,  $\text{Zn}^{2+}$ ,  $\text{Ni}^{2+}$ , and  $\text{Cd}^{2+}$  ions onto nonabsorbent are shown in Figs. 12–17.

#### 4.1.7. Ternary and quaternary component system

The adsorption isotherms for ternary and quaternary component systems were correlated to which the best model was fitted in binary component system. The parameters for each model obtained from nonlinear statistical fit of the equation to the experimental data.

The adsorption isotherms for ternary and quaternary component systems of  $\text{Cu}^{2+}$ ,  $\text{Ni}^{2+}$ ,  $\text{Zn}^{2+}$ , and  $\text{Cd}^{2+}$  ions onto nanosorbent are shown in Figs. 18–22. From these figures and tables (Tables 5 and 6), the following observation can be concluded:

- (1) For each the binary, ternary, and quaternary systems the combination of Langmuir–Freundlich model seems to give the best fit for the experimental data with highest value of  $R^2$ . It can be seen also that,  $\text{Cu}^{2+}$  always adsorbed more favorably onto nanosorbent than  $\text{Zn}^{2+}$ ,  $\text{Ni}^{2+}$ , and  $\text{Cd}^{2+}$  in binary, ternary, and quaternary systems.

Table 1  
Main physicochemical properties of the metals tested

Properties	Copper	Nickel	Cadmium	Zinc
Formula	Cu <sup>2+</sup> from Cu (NO <sub>3</sub> ) <sub>2</sub>	Ni <sup>2+</sup> from Ni (NO <sub>3</sub> ) <sub>2</sub>	Cd <sup>2+</sup> from Cd(NO <sub>3</sub> ) <sub>2</sub>	Zn <sup>2+</sup> from Zn (NO <sub>3</sub> ) <sub>2</sub>
Appearance	Blue crystals	Emerald green solid	White crystals	Colorless crystals
Molar mass (g mol <sup>-1</sup> )	241.6	290.79	236.42	297.49
Standard atomic weight	63.546	58.6934	112.414	65.38
Atomic radius (pm)	128	124	151	134
van der Waals radius (pm) <sup>a</sup>	140	163	158	139
Electronegativity (Pauling scale) <sup>b</sup>	1.9	1.91	1.69	1.65
Company	BDH (England)	Fluka (Switzerland)	RIEDEL-DE HAEN AG (Germany)	SCHARLAU (Spain)

<sup>a</sup>Pico meter = 10<sup>-12</sup> m.

<sup>b</sup>Pauling Scale: a dimensionless quantity, on a relative scale running from around 0.7 to 3.98 (Hydrogen was chosen as the reference, its electronegativity was fixed first at 2.1, later revised to 2.20).

Table 2  
The main physical properties of the nanosorbent

Physical properties of the nanosorbent, iron oxide (Fe <sub>3</sub> O <sub>4</sub> )	
Purity	98+%
Average particle size	20–30 nm
Surface area <sup>a</sup>	40–60 m <sup>2</sup> /g
Color dark	Dark brown
Morphology	Spherical
Bulk density	0.84 g/cm <sup>3</sup>
True density	4.8–5.1 g/cm <sup>3</sup>

<sup>a</sup>External and specific surface areas of the nanosorbent were measured. The results show that there is no significant difference between them. Results are 61, 63 m<sup>2</sup>/g, respectively. This indicates that the nanoadsorbents have no significant porosity and maintain a high external surface area. This is agrees with [43]. External surface areas were obtained by t-plot method and the specific surface areas obtained by BET method.

- (2) The decrease in adsorption capacity in binary and ternary systems compared with the single metal systems due to all metals with exception of copper ions, reflects the existence of a competition between the metals studied for the binding sites present in nanoparticle surfaces. It seems that the total metal adsorption capacity onto the nanoparticles decreases with increasing the number of metals present. This fact supports the assumed competition between metals for the nanoparticle binding sites and tends to decrease the relative amount of each adsorbed element. These results agreed with the results obtained by [43].

The metal removal efficiency of nanosorbent in single and mixed system was inhibited by the presence of the other heavy metals in the system. The removal efficiency of Cu<sup>2+</sup> in single system reduced from 100% to 96.1, 96.4, and 97.6%, respectively, in binary system with Zn<sup>2+</sup>, Cd<sup>2+</sup>, and Ni<sup>2+</sup> ions, while the removal efficiency of Cu<sup>2+</sup> in ternary system reduced to 96.26, 91.62, and 95%, respectively, with [Zn<sup>2+</sup> + Cd<sup>2+</sup>], [Zn<sup>2+</sup> + Ni<sup>2+</sup>], and [Cd<sup>2+</sup> + Ni<sup>2+</sup>], finally the removal efficiency of Cu<sup>2+</sup> reduced to 91.4% in quaternary system. The removal efficiency of Zn<sup>2+</sup> in single system reduced from 100% to 64.8, 88.6, and 96%, respectively, in binary system with Cu<sup>2+</sup>, Cd<sup>2+</sup>, and Ni<sup>2+</sup> ions, while the removal efficiency of Zn<sup>2+</sup> in ternary system reduced to 51, 49, and 81.8%, respectively, with [Cu<sup>2+</sup> + Cd<sup>2+</sup>], [Cu<sup>2+</sup> + Ni<sup>2+</sup>], and [Cd<sup>2+</sup> + Ni<sup>2+</sup>], finally the removal efficiency of Zn<sup>2+</sup> is reduced by 41.8% in quaternary system. The removal efficiency of Cd<sup>2+</sup> in single system reduced from 98.1% to 81, 64, and 88.6%, respectively, in binary system with Zn<sup>2+</sup>, Cu<sup>2+</sup>, and Ni<sup>2+</sup> ions, while the removal efficiency of Cd<sup>2+</sup> in ternary system reduced to 44, 63, and 47%, respectively, with [Zn<sup>2+</sup> + Cu<sup>2+</sup>], [Zn<sup>2+</sup> + Ni<sup>2+</sup>], and [Cu<sup>2+</sup> + Ni<sup>2+</sup>], finally the removal efficiency of Cd<sup>2+</sup> reduced to 36.8% in quaternary system. The removal efficiency of Ni<sup>2+</sup> in single system reduced from 82% to 61, 58.8, and 58%, respectively, in binary system with Zn<sup>2+</sup>, Cd<sup>2+</sup>, and Cu<sup>2+</sup> ions, while the removal efficiency of Ni<sup>2+</sup> in ternary system reduced to 41.92, 20, and 20.4%, respectively, with [Zn<sup>2+</sup> + Cd<sup>2+</sup>], [Zn<sup>2+</sup> + Cu<sup>2+</sup>], and [Cd<sup>2+</sup> + Cu<sup>2+</sup>], finally the removal efficiency of Ni<sup>2+</sup> reduced to 16.68% in quaternary system.

Table 3

Thermodynamic constants of adsorption obtained for Cu<sup>2+</sup>, Cd<sup>2+</sup>, Zn<sup>2+</sup>, and Ni<sup>2+</sup> ions adsorbed onto nanoadsorbent.

Metal	Temperature (K)	$\Delta G^\circ$ (kJ mol <sup>-1</sup> )	$\Delta H^\circ$ (kJ mol <sup>-1</sup> )	$\Delta S^\circ$ (j mol <sup>-1</sup> K <sup>-1</sup> )	R <sup>2</sup>
Cu <sup>2+</sup>	293	-2.23055	12.8	0.051	0.964
	308	-3.26050			
	323	-3.77921			
Cd <sup>2+</sup>	293	-0.9404	10.59	0.039	0.977
	308	-1.69034			
	323	-2.12666			
Zn <sup>2+</sup>	293	-1.57132	11.25	0.043	0.996
	308	-2.29944			
	323	-2.88714			
Ni <sup>2+</sup>	293	-0.0359	7.119	0.024	0.999
	308	-0.41427			
	323	-0.7686			

Table 4

Parameters of single solute isotherm for Cu<sup>2+</sup>, Zn<sup>2+</sup>, Ni<sup>2+</sup>, and Cd<sup>2+</sup> ions for nanosorbent

Model	Parameter	Metal ions			
		Cu <sup>2+</sup>	Zn <sup>2+</sup>	Ni <sup>2+</sup>	Cd <sup>2+</sup>
Langmuir $q = \frac{bq_m C_e}{1 + bC_e}$ [33]	$q_m$ (mg/g)	9.4223	8.5623	5.7933	11.698
	$b$ (L/mg)	0.4247	0.19	0.0639	0.0613
	R <sup>2</sup>	0.8143	0.81	0.86	0.865
Freundlich $q = KC_e^{1/n}$ [52]	$K$ (mg/g) (mg/L) <sup>(1/n)</sup>	3.544	2.479	0.9446	1.8751
	$n$	3.6695	3.1877	2.4801	2.4836
	R <sup>2</sup>	0.899	0.8537	0.8816	0.9217
Redlich–Peterson $q_e = \frac{K_{RP}C_e}{1 + a_{RP}C_e^{b_{RP}}}$ [53]	$k_{RP}$ (mg/g)	0.2138	0.1625	1.562e13	0.1569
	$a_{RP}$ (L/mg)	-0.2283	-0.2571	1.913e13	-0.3198
	$\beta$ (-)	0.00002	.000026	0.556	0.000006
	R <sup>2</sup>	0.5604	0.495	0.8807	0.768
Sips $q_e = \frac{K_s C_e^{\beta_s}}{1 + a_s C_e^{\beta_s}}$ [40]	$k_s$ (l/g)	0.46034	0.40273	0.05114	0.5227
	$\beta$	0.02268	0.0258	0.00684	0.0498
	$a_s$ (L/mg)	-0.8729	-0.859	-0.963	-0.772
	R <sup>2</sup>	0.877	0.848	0.865	0.902
Khan $q_e = \frac{q_{max} b_k C_e}{(1 + b_k C_e)^{a_k}}$ [54]	$q_m$ (mg/g)	0.6502	0.5597	0.34003	0.25353
	$b_k$ (L/mg)	513.204	113.107	12.7709	139.262
	$a_k$	0.728	0.686	0.59743	0.596
	R <sup>2</sup>	0.8887	0.8436	0.8714	0.9015
Toth $q_e = \frac{q_{max} b_T C_e}{[1 + (b_T C_e)^{n_T}]^{1/n_T}}$ [32]	$q_m$ (mg/g)	102.994	81.7608	44.5025	227.12
	$b_T$	736.78	20.39	0.4606	1.8023
	$n_T$	8.789	7.1183	5.2311	7.443
	R <sup>2</sup>	0.8908	0.8485	0.877	0.913



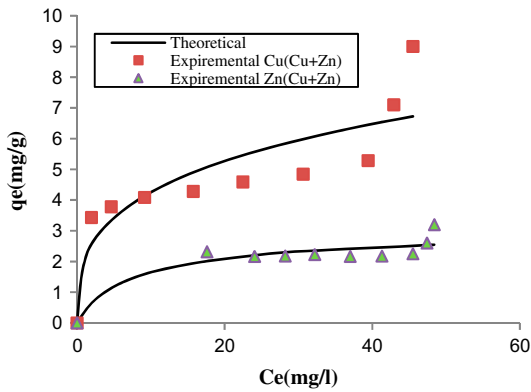


Fig. 12. Adsorption isotherms of copper and zinc ions onto nanosorbent,  $C_0(\text{Zn, Cu}) = 50 \text{ mg/L}$ .

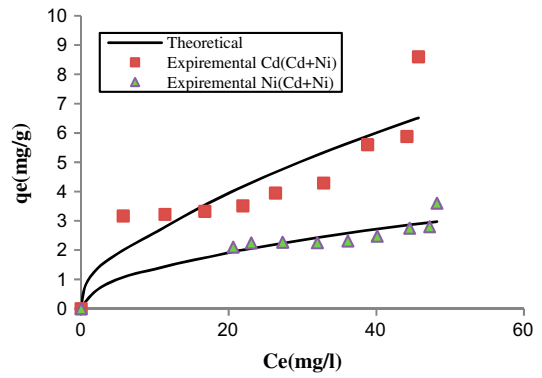


Fig. 15. Adsorption isotherms of cadmium and nickel ions onto nanosorbent,  $C_0(\text{Cd, Ni}) = 50 \text{ mg/L}$ .

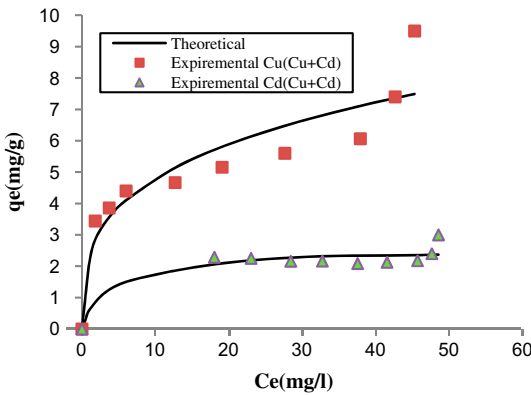


Fig. 13. Adsorption isotherms of copper and cadmium ions onto nanosorbent,  $C_0(\text{Cu, Cd}) = 50 \text{ mg/L}$ .

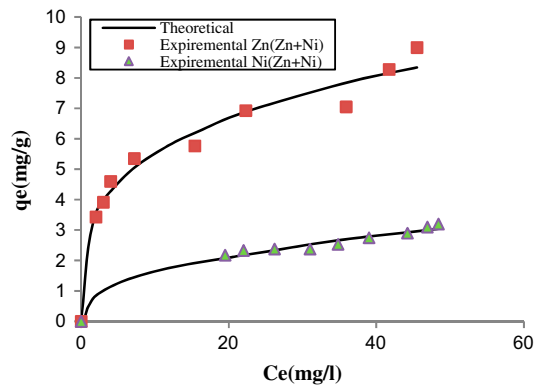


Fig. 16. Adsorption isotherms of zinc and nickel ions onto nanosorbent,  $C_0(\text{Zn, Ni}) = 50 \text{ mg/L}$ .

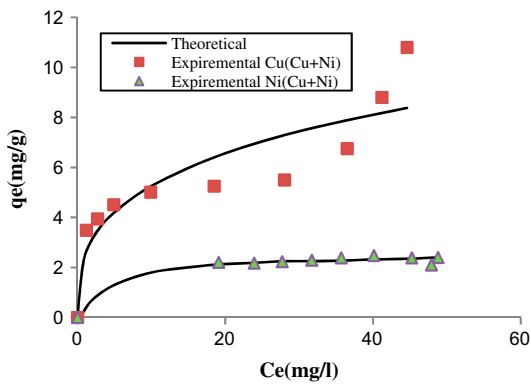


Fig. 14. Adsorption isotherms of copper and nickel ions onto nanosorbent,  $C_0(\text{Cu, Ni}) = 50 \text{ mg/L}$ .

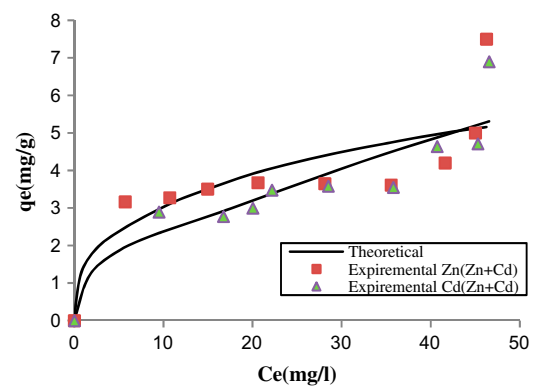


Fig. 17. Adsorption isotherms of zinc and cadmium ions onto nanosorbent,  $C_0(\text{Zn, Cd}) = 50 \text{ mg/L}$ .

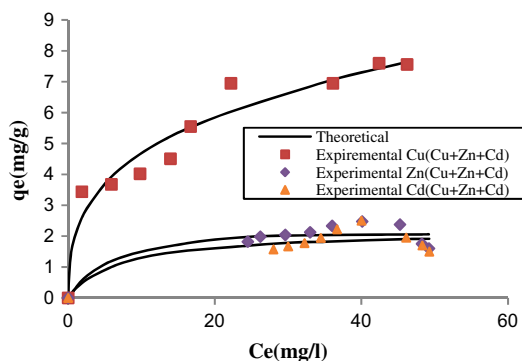


Fig. 18. Adsorption isotherms of copper, zinc, and cadmium ions onto nanosorbent,  $C_0(\text{Cu, Zn, Cd}) = 50 \text{ mg/L}$ .

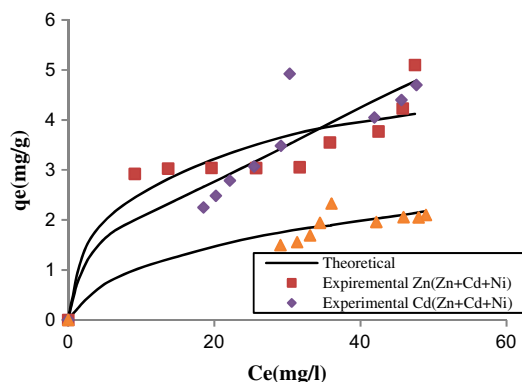


Fig. 21. Adsorption isotherms of zinc, cadmium, and nickel ions onto nanosorbent,  $C_0(\text{Zn, Ni, Cd}) = 50 \text{ mg/L}$ .

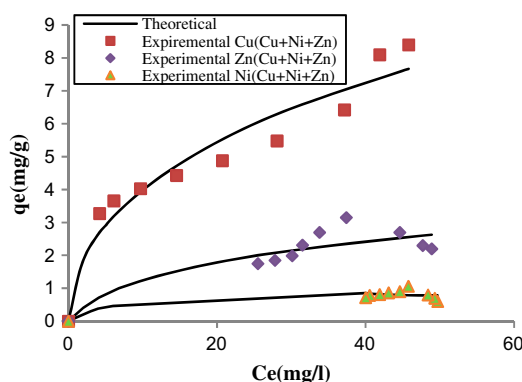


Fig. 19. Adsorption isotherms of copper, zinc and nickel ions onto nanosorbent,  $C_0(\text{Cu, Ni, Zn}) = 50 \text{ mg/L}$ .

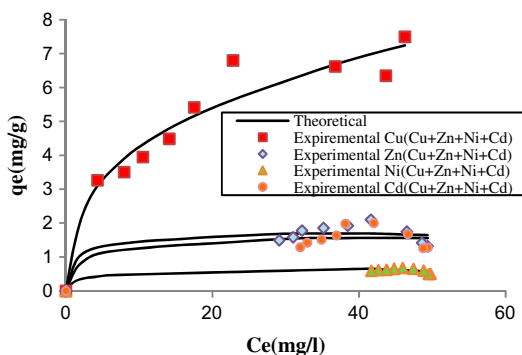


Fig. 22. Adsorption isotherms of copper, zinc, cadmium, and nickel ions onto nanosorbent,  $C_0(\text{Cu, Zn, Ni, Cd}) = 50 \text{ mg/L}$ .

## 5. Conclusions

### 5.1. Batch Process

#### 5.1.1. Single component system

- (1) Optimum pH was 6 for  $\text{Cu}^{2+}$ ,  $\text{Zn}^{2+}$ ,  $\text{Cd}^{2+}$ , and  $\text{Ni}^{2+}$  ions in the adsorption process onto  $\text{Fe}_3\text{O}_4$  nanoparticles.
- (2) The contact time to reach equilibrium for all heavy metals was 50 min.
- (3) The equilibrium isotherm was of favorable type and Freundlich model gave the best fit to the experimental data for this system.
- (4)  $\text{Cu}^{2+}$  ions was the most favorable component rather than  $\text{Zn}^{2+}$ ,  $\text{Cd}^{2+}$ , and  $\text{Ni}^{2+}$  ions, due to the lowest hydration van der Waals radius and higher electronegativities. The adsorption capacities were in the sequence of:  $\text{Cu}^{2+} > \text{Zn}^{2+} > \text{Cd}^{2+} > \text{Ni}^{2+}$ .

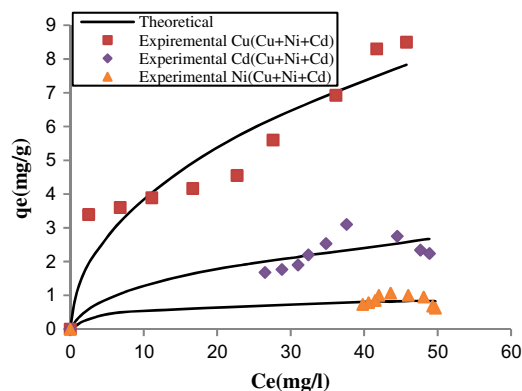


Fig. 20. Adsorption isotherms of copper, cadmium, and nickel ions onto nanosorbent,  $C_0(\text{Cu, Ni, Cd}) = 50 \text{ mg/L}$ .

- (5) The percentage removal efficiency was not altered greatly if the concentration between 10 and 50 mg/L, this was due to nanosorbent contains enough sites for adsorption, while between 100 and 150 mg/L the sites will not be enough so that the depletion in percentage removal efficiency was obvious.
- (6) Adsorption of  $\text{Cu}^{2+}$ ,  $\text{Zn}^{2+}$ ,  $\text{Cd}^{2+}$ , and  $\text{Ni}^{2+}$  ions was endothermic and physical in nature.

#### 5.1.2. Binary, ternary, and quaternary component system

- (1) Combination of Langmuir–Freundlich isotherm gave the best fit for the experimental data, and the equilibrium isotherm was of favorable type.
- (2) For each system  $\text{Cu}^{2+}$  ions was still most adsorbed component rather than  $\text{Zn}^{2+}$ ,  $\text{Cd}^{2+}$ , and  $\text{Ni}^{2+}$  ions.
- (3) Due to the competitive effect of  $\text{Cu}^{2+}$ ,  $\text{Zn}^{2+}$ ,  $\text{Cd}^{2+}$ , and  $\text{Ni}^{2+}$  ions with each other to occupy the available site (s) of the nanosorbent,  $\text{Cu}^{2+}$  ions offered the strongest component that able to displace  $\text{Zn}^{2+}$ ,  $\text{Cd}^{2+}$ , and  $\text{Ni}^{2+}$  ions from their sites, while  $\text{Ni}^{2+}$  ions was the weakest adsorbed component.
- (4) Compared with their adsorption in single component system the adsorption capacity of all four metals showed obvious decreases in the binary, ternary, and quaternary systems.
- (5) The percentage removal efficiency of each single component was decreased as each component presented with the other(s) in the binary, ternary, and quaternary system. This is due to the presence of more than one component will enhance the competitive struggling race for occupying a certain site.

#### References

- [1] S. Arivoli, Kinetic and Thermodynamic Studies on the Adsorption of Some Metal Ions and Dyes onto Low Cost Activated Carbons, Ph D. Thesis, Gandhigram Rural University, Gandhigram, 2007.
- [2] R. Ayyappan, A.C. Sophia, K. Swaminathan, S. Sandhya, Removal of Pb(II) from aqueous solution using carbon derived from agricultural wastes, *Process Biochem.* 40 (2005) 1293–1299.
- [3] M. Horsfall, A.I. Spiff, Equilibrium sorption study of Al(III) and Ag(II) in aqueous solutions by fluted pumpkin waste biomass, *Acta Chim. Slov.* 52 (2005) 174–181.
- [4] P. Lodeiro, R. Herrero, M.E. Sastre de Vicente, Batch desorption studies and multiple sorption–regeneration cycles in a fixed-bed column for Cd(II) elimination by protonated *Sargassum muticum*, *J. Hazard. Mater.* 137 (2006) 1649–1655.
- [5] G. Taghi, M. Khosravi, R. Rakhshae, Biosorption of Pb, Cd, Cu and Zn from the wastewater by treated *Azolla filiculoides* with  $\text{H}_2\text{O}_2/\text{MgCl}_2$ , *Int. J. Environ. Sci. Technol.* 1(4) (2005) 265–271.
- [6] M. Sahmoune, K. Louhab, A. Boukhiar, Biosorption of Cr(III) from aqueous solutions using bacterium biomass *Streptomyces rimosus*, *Int. J. Environ. Res.* 3(2) (2009) 229–238.
- [7] I.Z. Cheueh, Ion exchange modeling of silicotitanate column for chromium removal from argentine waste, Wisting house Savannah River Company, USA, 2005.
- [8] N.F. Gray, *Water Technology; An Introduction for Environmental Scientist's Engineers*, second ed., Elsevier, Butterworth-Heinemann, 2005.
- [9] M. Saleem, M.H. Chakrabarti, M.F. Irfan, S.A. Hajimolana, M.A. Hussain, Electro-kinetic remediation of nickel from low permeability soil, *Int. J. Electrochem. Sci.* 96 (2011) 4264–4275.
- [10] C. Quintelas, B. Fernandes, J. Castro, H. Figueiredo, T. Tavares, Biosorption of Cr(VI) by three different bacterial species supported on granular activated carbon—A comparative study, *J. Hazard. Mater.* 153 (2008) 799–809.
- [11] A.H. Sulaymon, K.W. Ahmed, Competitive adsorption of furfural and phenolic compounds onto activated carbon in fixed bed column, *Environ. Sci. Technol.* 42 (2) (2008) 392–397.
- [12] X. Huang, N.Y. Gao, Q.L. Zhang, Thermodynamics and kinetics of cadmium adsorption onto oxidized granular activated carbon, *J. Environ. Sci.* 19 (2007) 1287–1292.
- [13] M.R. Panuccio, A. Sorgonà, M. Rizzo, G. Cacco, Cadmium adsorption on vermiculite, zeolite and pumice: Batch experimental studies, *J. Environ. Manage.* 90 (2009) 364–374.
- [14] J. Hizal, R. Apak, Modeling of cadmium(II) adsorption on kaolinite-based clays in the absence and presence of humic acid, *Appl. Clay Sci.* 32 (2006) 232–244.
- [15] J.T. Bamgbose, S. Adewuyi, O. Bamgbose, A.A. Adetoye, Adsorption kinetics of cadmium and lead by chitosan, *Afr. J. Biotechnol.* 9 (2010) 2560–2565.
- [16] E.W. Shin, K.G. Karthikeyan, M.A. Tshabalala, Adsorption mechanism of cadmium on juniper bark and wood, *Bioresour. Technol.* 98 (2007) 588–594.
- [17] K. Sevgi, Adsorption of Cd(II), Cr(III) and Mn(II) on natural sepiolite, *Desalination* 244 (2009) 24–30.
- [18] G.C. Panda, S.K. Das, A.K. Guha, Biosorption of cadmium and nickel by functionalized husk of *Lathyrus sativus*, *Colloids Surf. B: Biointerfaces* 62 (2008) 173–179.
- [19] V. Srivastava, C.H. Weng, V.K. Singh, Y.C. Sharma, Adsorption of nickel ions from aqueous solutions by nano alumina: Kinetic, mass transfer, and equilibrium studies, *J. Chem. Eng. Data* 56 (2011) 1414–1422.
- [20] V.K. Gupta, S. Agarwal, T.A. Saleh, Synthesis and characterization of alumina coated carbon nanotubes and their application for lead removal, *J. Hazard. Mater.* 185 (2011) 17–23.

- [21] Y. Feng, J.L. Gong, G.M. Zeng, Q.Y. Niu, H.Y. Zhang, C.G. Niu, J.H. Deng, M. Yan, Adsorption of Cd(II) and Zn(II) from aqueous solutions using magnetic hydroxyapatite nanoparticles as adsorbents, *Chem. Eng. J.* 162 (2010) 487–494.
- [22] P. Xu, M.G. Zeng, L.D. Huang, L.C. Feng, S. Shuang, H.M. Zhao, C. Lai, Z. Wei, C. Huang, X.G. Xie, F.Z. Liu, Use of iron oxide nanomaterials in wastewater treatment: A review, *Sci. Total Environ.* 424 (2012) 1–10.
- [23] V.K. Gupta, A. Nayak, Cadmium removal and recovery from aqueous solutions by novel adsorbents prepared from orange peel and Fe<sub>2</sub>O<sub>3</sub> nanoparticles, *India Chem. Eng. J.* 180 (2012) 81–90.
- [24] J. Hu, G.H. Chen, I.M.C. Lo, Removal and recovery of Cr(VI) from wastewater by maghemite nanoparticles, *Water Res.* 39 (2005) 4528–4536.
- [25] Y.F. Shen, J. Tang, Z.H. Nie, Y.D. Wang, Y. Ren, L. Zuo, Preparation and application of magnetic Fe<sub>3</sub>O<sub>4</sub> nanoparticles for wastewater purification, *Sep. Sci. Technol.* 68 (2009) 312–319.
- [26] J.F. Liu, Z.S. Zhao, G.B. Jiang, Coating Fe<sub>3</sub>O<sub>4</sub> magnetic nanoparticles with humic acid for high efficient removal of heavy metals in water, *Environ. Sci. Technol.* 42 (2008) 6949–6954.
- [27] Z. Aksu, F. Gönen, Z. Demircan, Biosorption of chromium(VI) ions by Mowital®B30H resin immobilized activated sludge in a packed bed: Comparison with granular activated carbon, *Process Biochem.* 38 (2002) 175–186.
- [28] D. Kratochvil, B. Volesky, Advances in the biosorption of heavy metals, *Trends Biotechnol.* 16 (1998) 291–300.
- [29] M. J. Ridha, Competitive biosorption of heavy metals using expanded granular sludge bed reactor, Ph.D. Thesis, University of Baghdad, College of Engineering, 2011.
- [30] M.D. Mashitah, Y. Yus Azila, S. Bhatia, Biosorption of cadmium(II) ions by immobilized cells of *Pycnoporus sanguineus* from aqueous solution, *Bioresour. Technol.* 99 (2008) 4742–4748.
- [31] S. Basha, Z. Murthy, Kinetic and equilibrium models for biosorption of Cr(VI) on chemically modified seaweed *Cystoseira indica*, *Adv. Environ. Res.* 42(11) (2007) 1521–1529.
- [32] K. Vijayaraghavan, Y.S. Yun, Bacterial biosorbents and biosorption, *Biotechnol. Adv.* 26 (2008) 266–291.
- [33] C.C. Lin, Y.T. Lai, Adsorption and recovery of lead(II) from aqueous solutions by immobilized *Pseudomonas Aeruginosa* PU21 beads, *J. Hazard. Mater.* 137(1) (2006) 99–105.
- [34] T. Padmesh, K. Vijayaraghavan, G. Sekaran, M. Velan, Application of *Azolla rongpong* on biosorption of acid red 88, acid green 3, acid orange 7 and acid blue 15 from synthetic solutions, *Chem. Eng. J.* 122 (2006) 55–63.
- [35] W. Jianlong, C. Can, Adsorbents for heavy metals removal and their future, *Biotechnol. Adv.* 27 (2009) 195–226.
- [36] J. Wang, C. Chen, Biosorbents for heavy metals removal and their future, *Biotechnol. Adv.* 27 (2009) 195–226.
- [37] V. César, I. Joan, F. Adriana, L. José, Evaluating binary sorption of phenol/aniline from aqueous solutions onto granular activated carbon and hypercrosslinked polymeric resin (MN200), *Water Air Soil Pollut.* 210 (2010) 421–434.
- [38] A. Fahmi, K. Munther, Competitive adsorption of nickel and cadmium on sheep manure waste, experimental and prediction studies, *Sep. Sci. Technol.* 38(2) (2003) 483–497.
- [39] A.H. Sulaymon, B.A. Abid, J.A. Al-Najar, Removal of lead copper chromium and cobalt ions onto granular activated carbon in batch and fixed-bed adsorbents, *Chem. Eng. J.* 155(3) (2009) 647–653.
- [40] R. Sips, On the structure of a catalyst surface, *J. Chem. Phys.* 16 (1948) 490–495.
- [41] APHA, Standard Methods for the Examination of Water and Wastewater, 19th ed., American Public Health Association, Washington, DC, 1995.
- [42] J. Aldre, B. Morais, P. Shiva, D.L. Valderi, G.S. Antonio, Biosorption of heavy metals in upflow sludge columns, *Bioresour. Technol.* 98 (2007) 1418–1425.
- [43] N.N. Nassar, Rapid removal and recovery of Pb(II) from wastewater by magnetic nano-adsorbents, *J. Hazard. Mater.* 184 (2010) 538–546.
- [44] P.R. Grossl, D.L. Sparks, C.C. Ainsworth, Rapid kinetics of Cu(II) adsorption–desorption on goethite, *Environ. Sci. Technol.* 28 (1994) 1422–1429.
- [45] F. Çolak, N. Atar, A. Olgun, Biosorption of acidic dyes from aqueous solution by *Paenibacillus macerans*: Kinetic, thermodynamic and equilibrium studies, *Chem. Eng. J.* 150(1) (2009) 122–130.
- [46] S.M. Hasany, M.M. Saeed, M. Ahmed, Sorption and thermodynamic behavior of Zn(II)-thiocyanate complexes onto polyurethane foam from acidic solutions, *J. Radioanal. Nuclear Chem.* 252(3) (2002) 477–484.
- [47] B. Zubejde, C. Ercan, D. Mehmet, Equilibrium and thermodynamic studies on biosorption of Pb(II) onto *Candida albicans* biomass, *Hazard. Mater.* 161 (2009) 62–67.
- [48] V. Padmavathy, Biosorption of nickel(II) ions by baker's yeast: Kinetic, thermodynamic and desorption studies, *Bioresour. Technol.* 99 (2008) 3100–3109.
- [49] H.A. Hawari, N.C. Mulligan, Biosorption of lead(II), cadmium(II), copper(II) and nickel(II) by anaerobic granular biomass, *Bioresour. Technol.* 97 (2006) 692–700.
- [50] S.T. Manhan, Controlling heavy metal in water by adsorption, *Bio. Chem. J.* 60(7) (2005) 801–803.
- [51] K.H. Chong, B. Volesky, Metal biosorption equilibria in a ternary system, *Biotechnol. Bioeng.* 49(6) (1995) 629–638.
- [52] A. Öztürk, T. Artan, A. Ayar, Biosorption of nickel(II) and copper(II) ions from aqueous solution by *Streptomyces coelicolor*, A3(2), *Colloids Surf., B: Biointerfaces* 34(2) (2004) 105–111.
- [53] N.S. Maurya, A.K. Mittal, P. Cornel, E. Rother, Biosorption of dyes using dead macro fungi: Effect of dye structure, ionic strength and pH, *Bioresour. Technol.* 97 (2006) 512–521.
- [54] M.H. Khani, A.R. Keshtkar, B. Meysami, M.F. Zarea, R. Jalali, Biosorption of uranium from aqueous solutions by nonliving biomass of marine algae *Cystoseria indica*, *Electron. J. Biotechnol.* 9(2) (2006) 100–106.